
This is an electronic reprint of the original article.
This reprint may differ from the original in pagination and typographic detail.

Tuomisto, Filip; Mäki, Jussi-Matti; Svensk, Olli; Törmä, Pekka; Ali, Muhammad; Suihkonen, Sami; Sopanen, Markku

Defect studies with positrons: what could we learn on III-nitride heterostructures?

Published in:
Journal of Physics: Conference Series

DOI:
[10.1088/1742-6596/225/1/012057](https://doi.org/10.1088/1742-6596/225/1/012057)

Published: 01/01/2010

Document Version
Publisher's PDF, also known as Version of record

Published under the following license:
CC BY

Please cite the original version:
Tuomisto, F., Mäki, J.-M., Svensk, O., Törmä, P., Ali, M., Suihkonen, S., & Sopanen, M. (2010). Defect studies with positrons: what could we learn on III-nitride heterostructures? *Journal of Physics: Conference Series*, 225(1), 1-6. Article 012057. <https://doi.org/10.1088/1742-6596/225/1/012057>

This material is protected by copyright and other intellectual property rights, and duplication or sale of all or part of any of the repository collections is not permitted, except that material may be duplicated by you for your research use or educational purposes in electronic or print form. You must obtain permission for any other use. Electronic or print copies may not be offered, whether for sale or otherwise to anyone who is not an authorised user.

Defect studies with positrons: What could we learn on III-nitride heterostructures?

This content has been downloaded from IOPscience. Please scroll down to see the full text.

2010 J. Phys.: Conf. Ser. 225 012057

(<http://iopscience.iop.org/1742-6596/225/1/012057>)

View [the table of contents for this issue](#), or go to the [journal homepage](#) for more

Download details:

IP Address: 130.233.216.246

This content was downloaded on 08/06/2017 at 07:07

Please note that [terms and conditions apply](#).

You may also be interested in:

[Vacancy defects in III-nitrides: what does positron annihilation spectroscopy reveal?](#)

Filip Tuomisto

[Positron Annihilation Spectroscopy on Nitride-Based Semiconductors](#)

Akira Uedono, Shoji Ishibashi, Nagayasu Oshima et al.

[Characterization of helium bubbles in Si by slow positron beam](#)

M Maekawa and A Kawasuso

[Cation vacancies and electrical compensation in Sb-doped thin-film SnO₂ and ZnO](#)

E Korhonen, V Prozheeva, F Tuomisto et al.

[Determination of defect content and defect profile in semiconductor heterostructures](#)

A Zubiaga, J A Garcia, F Plazaola et al.

[Identification of vacancy defect complexes in transparent semiconducting oxides ZnO, In₂O₃ and SnO₂](#)

Iija Makkonen, Esa Korhonen, Vera Prozheeva et al.

[Doppler broadening of annihilation radiation of some single-element materials from the second to the sixth periods](#)

A Kawasuso, M Maekawa and K Betsuyaku

[Free volume in Zr-based bulk glassy alloys studied by positron annihilation techniques](#)

A Ishii, A Iwase, Y Yokoyama et al.

[Evaluation of stainless steel under tensile stress using positron microbeam](#)

M Maekawa, Y Yabuuchi and A Kawasuso

Defect studies with positrons: what could we learn on III-nitride heterostructures?

Filip Tuomisto¹, Jussi-Matti Mäki¹, Olli Svensk², Pekka T. Törmä², Muhammad Ali², Sami Suihkonen², and Markku Sopanen²

¹Department of Applied Physics, Aalto University, P.O. Box 11100, FI-00076 Aalto Espoo, Finland

²Department of Micro and Nanosciences, Aalto University, P.O. Box 13500, FI-00076 Aalto Espoo, Finland

filip.tuomisto@tkk.fi

Abstract. We have applied positron annihilation spectroscopy to study 400 – 500 nm InGaN-based LED structures, as well as InGaN and AlGaN materials with varying In and Al contents. We find that the effect of adding In to GaN on the annihilation parameters obeys the Vegard's law, while in the case of AlGaN the possible effect of Al is completely screened by efficient formation of cation vacancies. The results obtained in the InGaN LED structures are indistinguishable from defect-free GaN, suggesting that the positrons annihilate preferentially in the barriers of the MQW system.

1. Introduction

In device structures fabricated out of III-nitrides (alloys of AlN, GaN and InN) the structural quality of both the semiconductor materials themselves and the heterointerfaces between them often limit significantly the output due to the unfortunate aspect of having lattice constants that differ considerably one from another. In addition to extended defects such as stacking faults or dislocations, point defects have a significant impact on the electrical and optical properties of the nitride semiconductor materials. Positron annihilation spectroscopy is a method that is particularly well suited for studying vacancy defects in semiconductors. During the past decade it has been applied in numerous studies where the identities, concentrations and characteristics of both in-grown and processing-induced vacancy defects in nitride semiconductors have been determined, see e.g. [1–8] and the references therein.

In this work we apply positron annihilation spectroscopy to study InGaN light emitting device (LED) structures (wavelengths 400 – 500 nm), as well as InGaN and AlGaN materials with different In and Al contents, respectively. We interpret the data based on earlier results [6–11] obtained in GaN, InN, and AlN and the cation (group III) vacancies in these materials.

2. Experimental details

The positron annihilation characteristics were measured in thin epitaxial films and device structures by using a mono-energetic continuous positron beam. As lifetime experiments are not possible with a

continuous beam, the Doppler broadening of the annihilation radiation was monitored as a function of the beam energy, providing a depth profile of the signal. The motion of the annihilating electron-positron pair causes a Doppler shift in the annihilation radiation $\Delta E = cp_L / 2$, where p_L is the longitudinal momentum component of the pair in the direction of the annihilation photon emission. This causes the broadening of the 511 keV annihilation line. The shape of the 511 keV peak gives thus the one-dimensional momentum distribution $\rho(p_L)$ of the annihilating electron-positron pairs. A Doppler shift of 1 keV corresponds to a momentum value of $p_L = 0.54$ a.u. ($\approx 3.91 \times 10^{-3} m_0c$).

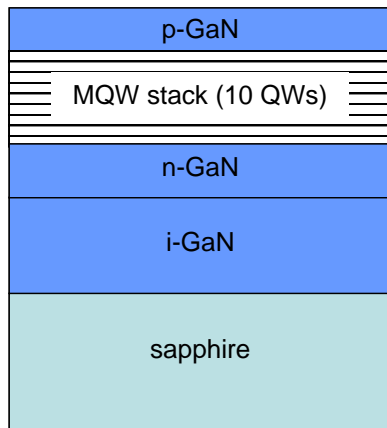


Figure 1. Schematic representation of the relevant parts of the LED structures studied in this work. The initial layer of nominally undoped GaN (i-GaN) is 2 μm thick, the n-type doped GaN layer is 1 μm thick, and the p-GaN electron blocking layer is 200 nm thick. The active MQW area consists of 10 InGaN well – GaN barrier pairs, where the well thickness is 4 nm and barrier thickness 25 nm, hence the total thickness of the MQW stack is 290 nm.

The Doppler broadening can be experimentally measured using a Ge gamma ray detector with a good energy resolution. The typical resolution of a detector is around 1–1.5 keV at 500 keV. This is considerable compared to the total width of 2–3 keV of the annihilation peak meaning that the experimental lineshape is strongly influenced by the detector resolution. Therefore, various shape parameters are used to characterize the 511 keV line. The low electron-momentum parameter S is defined as the ratio of the counts in the central region (typically $p_L < 0.4$ a.u.) of the annihilation line to the total number of the counts in the line. In the same way, the high electron-momentum parameter W is the fraction of the counts in the wing regions of the line (typically $p_L > 1.5$ a.u.). Due to their low momenta, mainly valence electrons contribute to the region of the S parameter. On the other hand, only core electrons have momentum values high enough to contribute to the W parameter. Therefore, S and W are sometimes called the valence and core annihilation parameters, respectively.

The high-momentum part of the Doppler broadening spectrum arises from annihilations with core electrons that contain information on the chemical identity of the atoms. Thus the detailed investigation of core electron annihilation can reveal the nature of the atoms in the regions where positrons annihilate. In order to study the high-momentum part in detail, the experimental background needs to be reduced. A second gamma ray detector can be placed opposite to the Ge detector and the only events that are accepted are those for which both 511 keV photons are detected [12, 13]. Depending on the type of the second detector, electron momenta even up to $p \approx 8$ a.u. ($\approx 60 \times 10^{-3} m_0c$) can be measured with the coincidence detection of the Doppler broadening.

The nitride thin films and device structures studied in this work were grown by metal-organic vapor phase epitaxy (MOVPE) directly on sapphire substrates. For further details about the growth procedures, see Refs. [14–16]. We studied $\text{In}_x\text{Ga}_{1-x}\text{N}$ and $\text{Al}_x\text{Ga}_{1-x}\text{N}$ alloys with In and Al contents ranging from up to 22 % and 25 %, respectively. The device structures were realistic LED structures corresponding to wavelengths in the 400–500 nm, with In content varying from 5 % to 15 % in the quantum wells (QWs) in the active area consisting of a multi-quantum-well system of 10 well-barrier pairs. The schematic of the LED structures is shown in Fig. 1.

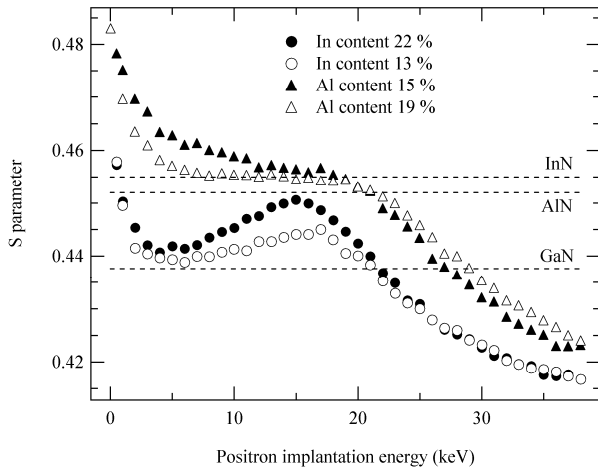


Figure 2. The S parameter measured as a function of positron implantation energy in selected $\text{In}_x\text{Ga}_{1-x}\text{N}$ and $\text{Al}_x\text{Ga}_{1-x}\text{N}$ layers grown by MOVPE on sapphire. The dashed lines show the characteristic S parameters of GaN, InN and AlN.

3. InGaN and AlGaN layers

Figure 2 shows the S parameter measured at room temperature as a function of positron implantation energy in selected $\text{In}_x\text{Ga}_{1-x}\text{N}$ and $\text{Al}_x\text{Ga}_{1-x}\text{N}$ samples. When positrons are implanted close to the sample surface with $E = 0 - 1$ keV, a relatively high S parameter of $S = 0.46$ ($S = 0.48$) is recorded in the $\text{In}_x\text{Ga}_{1-x}\text{N}$ ($\text{Al}_x\text{Ga}_{1-x}\text{N}$) samples. These values characterize the defects and chemical nature of the near-surface region of the samples at the depth $0 - 5$ nm. The region of constant S gives the characteristic value of the $\text{Al}_x\text{Ga}_{1-x}\text{N}$ layer and extends up to 20 keV in the thickest sample. In the $\text{In}_x\text{Ga}_{1-x}\text{N}$ layers, the S parameter increases strongly toward the layer/substrate interface, indicating that the material is different close to the interface. The decrease of the S parameter at higher implantation energies is due to the increasing fraction of positrons annihilating in the sapphire substrate, for which the characteristic S parameter is roughly $S = 0.41$. It is clearly seen that the S parameter of the layer increases with increasing content of either In or Al in the nitride lattice.

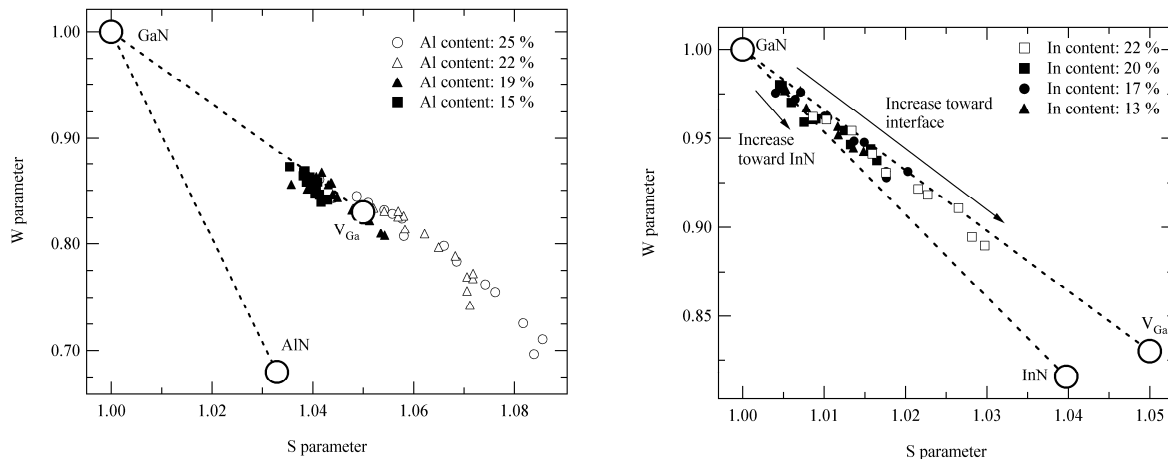


Figure 3. The relative S and W parameters (divided by the values characteristic to GaN) measured in the $\text{Al}_x\text{Ga}_{1-x}\text{N}$ (a) and $\text{In}_x\text{Ga}_{1-x}\text{N}$ (b) layers. Data points corresponding to the GaN, InN and AlN lattice and the Ga vacancy in GaN are also shown.

The characteristic S parameters of InN and AlN, determined from well-defined reference samples [6, 11] are significantly higher than that of GaN. However, as can be seen in figure 3a, the reason for the increase in $\text{Al}_x\text{Ga}_{1-x}\text{N}$ layers is enhanced annihilation in group III vacancies. On the other hand, the increase in the S parameter far away from the interface in the $\text{In}_x\text{Ga}_{1-x}\text{N}$ layers is quite close to what

one would expect if the S parameter is assumed to be given by a linear combination of the S parameters of InN and GaN with the fractions given directly by the In content. The strong increase in the S parameter toward the layer/sapphire interface is due to enhanced trapping at group III vacancies abundant near the interface, as can be seen in figure 3b, and not due to an inhomogeneous In distribution. A similar effect can be observed in epitaxial vapor-phase GaN grown directly on sapphire [17,18]. Hence it would seem that there is no preference for positrons to annihilate in either locally In-rich or In-poor regions in the lattice. Interestingly, in recent state-of-the-art first principles calculations [19], it is shown that in polar nitride superlattices positrons always prefer to annihilate in pure GaN instead of areas with In or Al, while the situation is less clear in non-polar structures, even if the positron affinity is the lowest for GaN (compared to InN and AlN).

4. LED structures

In addition to the bandgap modulation that is essential for the electronic device, the use of different nitrides creates electric fields in the structure induced by spontaneous polarization due the non-inversionsymmetric wurtzite structure of the materials [20–22]. These electric fields are bound to affect the positron localization in a similar manner as the electron and hole localization. Indeed, recent theoretical calculations show that in a polar structure the positron localize at the well-barrier interface in a nitride heterostructure [19]. Figure 4 shows a schematic representation of the situation. In more detail, the positron doesn't actually localize exactly at the interface, but on the GaN side in such a way that more than 90 % of the positron density is in the GaN layer and less than ten 10 % in the In- or Al-containing layer. Further, the positron affinity is favorable in GaN (compared to InN and AlN) and hence even in non-polar structures, where the polarization-induced electric field is missing, positrons localize in the GaN layer (but the distribution is wider and centered at the center of the layer, not near an interface).

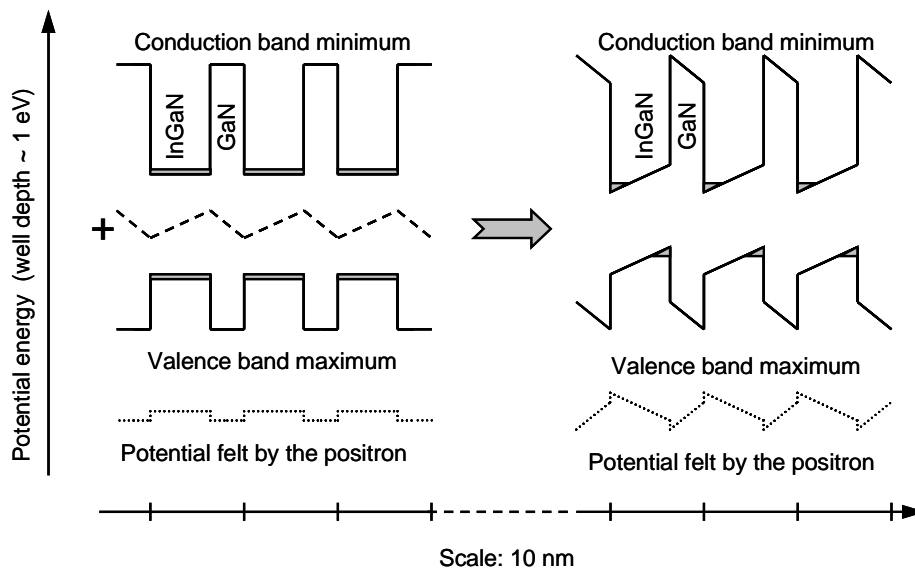


Figure 4. Schematic representation of the polarization-induced electric field on positron localization.

Figure 5 shows the S parameter measured as a function of energy at room temperature in the InGaN LED structures. The data are very clear: no traces of In are observed in the data from the MQW depths (shaded area in the figure), indicating that positrons do not annihilate in In-rich surroundings to a measurable extent. The data coincide with defect-free (i.e., no defects detected with positrons) GaN, and in fact the vacancy concentrations in the barrier GaN seem to be even lower than that in the n-

GaN on which the LED structure is grown, as the S parameter increases at higher positron implantations energies.

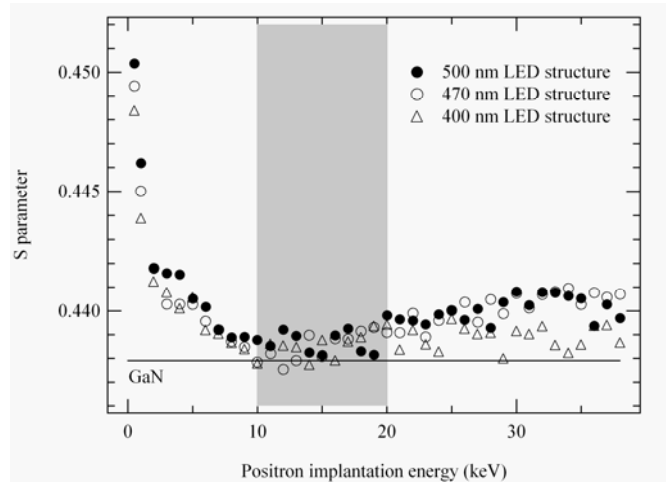


Figure 5. The S parameter measured as a function of positron implantation energy at room temperature in the LED structures. The grey area shows the MQW range of depths.

Finally, it is important to note that the above interpretations of the experimental data concerning the preference of positrons to annihilate in pure GaN or In- and Al-rich regions hold only when the crystal lattice is otherwise intact. When group III-vacancy defects are present, the sensitivity to the immediate surrounding of the positron annihilation site is lost, as the positron “feels” predominantly the nitrogen atoms immediately neighbouring the vacancy. In fact, the above-mentioned theoretical calculations also show that the preference of GaN over AlN and InN is lost when group III vacancies are introduced in the lattice, irrespective of the location of the vacancy (in any of the nitrides or at the interface), and the positrons localize at the vacancy.

5. Summary

In summary., we have applied positron annihilation spectroscopy to study 400 – 500 nm InGaN-based LED structures, as well as InGaN and AlGaIn materials with varying In and Al contents. We find that the effect of adding In to GaN on the annihilation parameters is close to that what one could expect from Vegard’s law, while in the case of AlGaIn the effect of Al is completely screened by efficient formation of cation vacancies. The results obtained in the InGaIn LED structures are indistinguishable from defect-free GaN, suggesting that the positrons annihilate preferentially in the barriers of the MQW system, in good agreement with recent theoretical predictions.

Acknowledgments

This work has been partially funded by the Academy of Finland. We acknowledge the support of the Multidisciplinary Institute of Digitalization and Energy (MIDE) of the Helsinki University of Technology.

References

- [1] Saarinen K, Laine T, Kuisma S, Nissilä J, Hautojärvi P, Dobrzynski L, Baranowski J M, Pakula K, Stepniewski R, Wojdak M, Wyszomolek A, Suski T, Leszczynski M, Grzegory I and Porowski S 1997 *Phys. Rev. Lett.* **79** 3030
- [2] Tuomisto F, Suski T, Teisseyre H, Krysko M, Leszczynski M, Lucznik B, Grzegory I, Porowski S, Wasik D, Witowski A, Gebicki W, Hageman P and Saarinen K 2003, *phys. status solidi (b)* **240** 289
- [3] Tuomisto F, Saarinen K, Lucznik B, Grzegory I, Teisseyre H, Suski T, Porowski S, Hageman P R and Likonen J 2005 *Appl. Phys. Lett.* **86** 031915
- [4] Hautakangas S, Ranki V, Makkonen I, Puska M J, Saarinen K, Xu X and Look D C 2006 *Phys. Rev. B* **73** 193301

- [5] Paskova T, Hommel D, Paskov PP, Darakchieva V, Monemar B, Bockowski M, Suski T, Grzegory I, Tuomisto F, Saarinen K, Ashkenov N, Schubert M 2006 *Appl. Phys. Lett.* **88** 141909
- [6] Tuomisto F, Pelli A, Yu K M, Walukiewicz W and Schaff W 2007 *Phys. Rev. B* **75** 193201
- [7] Tuomisto F, Paskova T, Kröger R, Figge S, Hommel D, Monemar B and Kersting R 2007 *Appl. Phys. Lett.* **90** 121915
- [8] Tuomisto F, Ranki V, Look D C and Farlow G C 2007 *Phys. Rev. B* **72** 165207
- [9] Oila J, Kemppinen A, Laakso A, Saarinen K, Egger W, Liskay L, Sperr P, Lu H and Schaff W J 2004 *Appl. Phys. Lett.* **84** 1486
- [10] Pelli A, Saarinen K, Tuomisto F, Ruffenach S and Briot O 2006 *Appl. Phys. Lett.* **89** 011911
- [11] Tuomisto F, Mäki J-M, Chemekova T Yu, Makarov Yu N, Avdeev O V, Mokhov E N, Segal A S, Ramm M G, Davis S, Huminic G, Helava H, Bickermann M and Epelbaum B M 2008 *J. Crystal Growth* **310** 3998
- [12] Alatalo M, Kauppinen H, Saarinen K, Puska M J, Mäkinen J, Hautojärvi P and Nieminen R M: 1995 *Phys. Rev. B* **51** 4176
- [13] Asoka-Kumar P, Alatalo M, Ghosh V J, Kruseman A C, Nielsen B and Lynn K G 1996 *Phys. Rev. Lett.* **77** 2097
- [14] Lang T, Odnoblyudov M A, Bougrov V E, Suihkonen S, Svensk O, Törmä P T, Sopenan M, Lipsanen H 2007 *J. Crystal Growth* **298** 276
- [15] Suihkonen S, Svensk O, Törmä P T, Ali M, Sopenan M, Lipsanen H, Odnoblyudov M A, Bougrov V E 2008 *J. Crystal Growth* **310** 1777
- [16] Svensk O, Törmä P T, Suihkonen S, Ali M, Lipsanen H, Sopenan M, Odnoblyudov M A, Bougrov V E 2008 *J. Crystal Growth* **310** 5154
- [17] Oila J, Kivioja J, Ranki V, Saarinen K, Look D C, Molnar R J, Park S S, Lee S K, Han J Y 2003 *Appl. Phys. Lett.* **82** 3422
- [18] Tuomisto F, Saarinen K, Bockowski M, Suski T, Paskova T and Monemar B 2006 *J. Appl. Phys.* **99** 066105
- [19] Makkonen I, Snicker A, Mäki J-M, Tuomisto F and Puska M J, submitted.
- [20] Bernardini F, Fiorentini V and Vanderbilt D 1997 *Phys. Rev. B* **56** R10024
- [21] Lefebvre P, Morel A, Gallart M, Taliercio T, Allegre J, Gil B, Mathieu H, Damilano B, Grandjean N and Massies J 2001 *Appl. Phys. Lett.* **78** 1252
- [22] Bernardini F and Fiorentini V 1998 *Phys. Rev. B* **57** R9427